ORIGINAL PAPER

Research on Bearing Mechanism and Spatial Layout Designing Parameters of Arch Support in Large Section Tunnel

Hui Qi · Wei Lu · Tiantao Zhang · Hongbin Chen · Zhaoming Chi · Shuo Xu · Peng Zhang

Abstract At present, there is no unified support design criterion for the construction of super-large cross-section tunnel. The design of initial supporting components is based on engineering analogy method, lacking theoretical and experimental guidance. The spacing of arch and longitudinal connection strength have significant influence on the bearing capacity of initial support system, so in-depth study in this area is very important. Therefore, based on the typical super-large cross-section tunnel-Letuan Tunnel of Binlai Expressway in China, laboratory test and numerical test are carried out in this paper to study the combinational bearing mechanism of multiple spatial arches in initial supporting system. This paper also clarifies the mechanical characteristics of spatial supporting system and the influence mechanism different designing parameters such as arch spacing, longitudinal connection spacing. The cost performance of each design scheme of the spatial supporting arch system is established. The research results show that the influence of arch spacing and longitudinal connection spacing on arch bearing capacity is remarkable. Strength of combined arch structures is 3.14–3.92 times of single arch frame. The influence of arch spacing is more obvious than that of longitudinal connection spacing. The research results can provide reference for related projects.

Keywords Super large section tunnel · Initial support system · Spatial combinational arch support · Support design

H. Qi
Qilu Transportation Development Group Co., Ltd., Jinan 250101, China

W. Lu (✉) · H. Chen · S. Xu · P. Zhang
Research Center of Geotechnical and Structural Engineering, Shandong University, Jinan 250061, China
e-mail: adam_luv@163.com

T. Zhang · Z. Chi
Qilu Transportation Construction Management Co., Jinan 250101, China

1 Introduction

It has become an important direction for the future world to fully utilize and develop underground space (Sharifzadeh et al. 2013). In recent years, the scale of highway construction is expanding day by day, and the number of super-large section highway tunnels such as one-way four-lane highway and two-way eight-lane highway tunnels is increasing rapidly. However, due to the large span, low flatness, complex construction procedures, multiple disturbances of surrounding rock and other problems, the initial support components are easy to lose stability or even failed directly, resulting in caving and even collapse. The main reason for the above-mentioned disasters is that there is no unified design and construction criterion for super-large

section tunnels at present. The engineering design is mostly based on engineering analogy method. While the construction cases of super-large cross-section tunnels are few, the applicability of engineering analogy is insufficient, and the research of bearing mechanism and mechanical characteristics of arch support for super-large cross section tunnels are also insufficient.

Some scholars have carried out theoretical and experimental research on arch support in the initial support system, but there is little research on the super-large section tunnel. Liping et al. (2012) carried out large-scale three-dimensional model tests in order to study the deformation mechanism of surrounding rock of super-large section tunnel in soft and fractured stratum under different construction methods and technology combinations to reveal the deformation and failure mechanism of surrounding rock. Kun et al. (2012) studied the double-section tunnel through the establishment of discrete element numerical simulation analysis model. Under the three construction schemes of side-wall heading method, CRD method and CD method, the regularity of the vault settlement, the horizontal displacement of the middle rock column, the horizontal displacement of the surrounding rock and the plastic zone of the surrounding rock are analyzed. The construction schemes of the different tunnels are optimized. Tiezhu (2015) studied the mechanical response characteristics of surrounding rock of super-large cross-section tunnel with small clearance based on the analysis of deformation and stress monitoring data of CRD tunnel and double-sidewall heading method construction section; Zheng-bin et al. (2006) analyzed the plastic zone distribution caused by large cross-section tunnel excavation based on numerical simulation results. Distribution of plastic zone, deformation characteristics and mechanism of surrounding rock of tunnel excavated by different construction methods are obtained; Qing-biao et al. (2013) studied the influence of different excavation methods on stratum and surrounding rock of close overlapping tunnel, the deformation and stress–strain evolution law of overlapping zone surrounding rock and existing tunnel lining under different excavation methods are revealed. The theoretical basis is provided for deformation control, support design and excavation optimization design of underground works. Gui-Jun (2005) used discrete element method to analyze the interaction between surrounding rock and

supporting structure of large cross-section tunnel in jointed fractured rock mass and the mechanical state of construction process. The numerical results are in good agreement with the measured data.

The above research shows that the deformation and failure of surrounding rock of large section tunnel are various and the mechanism is complex, which brings great difficulties to the safe construction of tunnel.

In the development of underground engineering stability control, the introduction of NATM has made bolt-mesh shotcrete support widely used, and it is the conventional support method of underground engineering currently. In order to increase support strength, the combined support method composed of steel arch and anchor bolt and shotcrete is widely used. Some scholars have conducted in-depth research on the mechanical properties and deformation characteristics of the steel arch support structure (Li-chao et al. 2013; Kezhong et al. 2014; Dehua et al. 2015; Ranjbarnia et al. 2018; Høiena et al. 2019). Some scholars have developed new types of arch support for underground engineering (He et al. 2014; ANDERS 2005; Wang et al. 2016; Wang et al. 2017; Kang et al. 2014). He et al. (2014) presents an innovation work on the development of a novel energy-absorbing bolt characterized by an extraordinarily large elongation and high constant resistance. The analytical work in this study provides solutions in the assessment of the large deformation and establishment of the forewarning precursors associated with deep mines. Wang et al. (2016) and (2017) proposed the confined concrete support system and studied in depth on the mechanical properties and failure mechanism of confined concrete arch, which provides a high-strength, economical and practical support theory for the difficulties of surrounding rock control in underground engineering.

However, the above research mainly concentrates on the bearing mechanism of single arch support. The research on the stability of arch under spatial combination condition is still insufficient, and there is few relevant research on the initial support system design of super-large section tunnel. Therefore, in order to further clarify the mechanical characteristics of the initial support arch and obtain the relevant design methods, relying on the typical super-large section tunnel project, this paper carried out a laboratory test and a numerical test of the bearing characteristics of the initial support arch under the spatial combinational state, and obtained the influence mechanism of the

arch parameters by changing the space layout parameters, which is the design basis of initial support system. The research results can provide reference for related engineering construction.

2 Typical Engineering Case

Magongci Tunnel of Bin Lai Expressway in China is a two-way eight-lane tunnel. The tunnel is located in a region with developed faults, serious rock weathering, widespread distribution of weak interbeds, a small amount of karst fissure water, serious eccentric pressure at the entrance of the tunnel, which is extremely unfavorable to the stability of the tunnel. The National Forest Park, wetland park and large reservoir water sources which the tunnel passes through have strict requirements on tunnel settlement. If the support strength is insufficient, it is easy to cause tunnel collapse and instability of the construction face (Fig. 1).

The original design scheme of the tunnel adopts the initial support system of bolt mesh shotcrete, in which the arch adopts I20b steel arch frame, the longitudinal spacing of the arches is 120 cm, and the adjacent arches are connected by longitudinal connecting steel bars with diameter of 25 mm, and the spacing of longitudinal connection is 150 cm.

3 Analysis of Bearing Capacity of Single Arch Support

In order to clarify the load-bearing mechanism and mechanical characteristics of supporting arch, this paper studied single arch based on the combination of laboratory test and numerical test.

3.1 Test Situation

3.1.1 Laboratory Test

3.1.1.1 Testing System The laboratory test of arch frame is completed based on the large-scale mechanical test system of arch support. The test system is mainly composed of four parts: frame reaction system, loading control system, data monitoring and acquisition system and load distribution system.

1. The frame reaction system is a three-storied steel structure modular assembling frame with an outer diameter of 20.5 m, an inner diameter of 16.5 m and a height of 6 m. It can provide 7200t reaction force with high strength, high stiffness and good stability. It can realize full scale mechanical test of supporting structure of super-large section underground engineering, it also adjusts to different shape of tunnel cross section using the assembling module.

2. The loading control system is mainly composed of 12 hydraulic pumping stations, 36 sets of oil cylinders, and servo control systems. Each hydraulic pump station has a maximum pressure of 25 MPa, and every three groups of parallel cylinders share one hydraulic station. Each loading channel is independent of each other. The 36-channel full servo hydraulic gradient loading-holding-loading control can be realized.
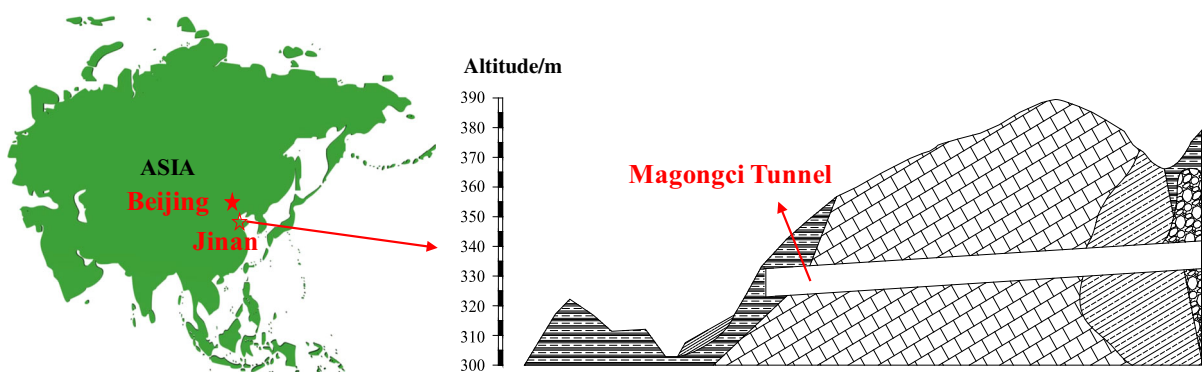

Fig. 1 Location of Magongci Tunnel

Fig. 2 Large mechanical test system for supporting structure of underground arch

3. The real-time data monitoring and acquisition system is composed of built-in high-precision force sensor, thermocouple sensor, multi-parameter automatic measurement system, computer control and display system. It can realize high-speed automatic monitoring of force, strain and displacement and real-time data acquisition. It can output and draw various experimental curves according to all kinds of needs.

4. The load transfer system consists of a compression bar, a transfer sleeve, a loading beam and a transfer rubber. The hydraulic cylinder is linked with the reaction frame through the pressure bar, and the length of the pressure bar can be adjusted according to the size of the test object.

The force transfer sleeve can adjust the cylinder's concentric force to ensure that the loading direction is radially perpendicular to the outer contour of the arch to achieve radial pressure. Loading beam can transfer the concentrated force produced by the cylinder to a wider range. Adding force-transfer rubber between the loading beam and the test object can further expand the contact surface between the two, so as to realize flexible loading to prevent local premature failure of the test object caused by stress concentration and affect the overall test results (Fig. 2).

3.1.1.2 Testing Specimen Based on the engineering design scheme, the test arch adopts the three-center inverted arch type, and its shape and the specific size of the joint members are shown in the Fig. 3.

3.1.1.3 Loading Scheme The test loading cylinder is composed of 12 groups of cylinders F1 ∼ F12, each of
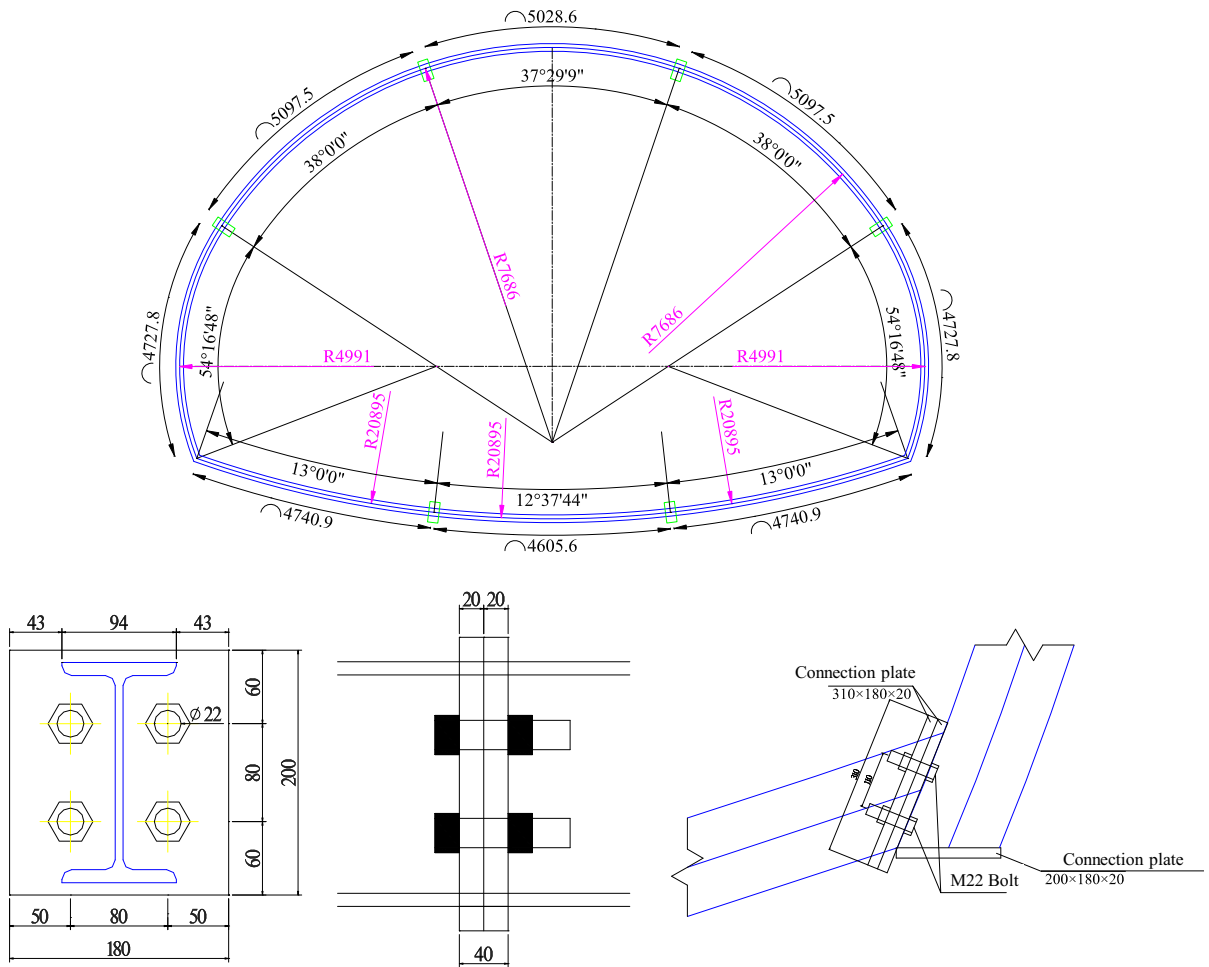
Fig. 3 Arch and connection component

which is composed of two cylinders. The cylinder is loaded on the arch through the loading beam.

The loading mode adopts three-stage compressive loading, the initial loading rate is set at 0.3 kN/s, and the initial loading rate is set at 1 min per 10 kN. When the load is greater than 60% of the predicted failure load, the loading rate is adjusted to 0.2 kN/s, and every 5 kN for 1 min. When the load is greater than 90% of the predicted failure load, the loading rate is adjusted to 0.1 kN/s, and every 2 kN for 0.5 min. The test ends when the arch frame enters the yield state, local instability or obvious damage.

3.1.1.4 Monitoring In order to study the overall deformation and local yield instability of the arch frame, the specific measuring points are arranged as shown in the figure. Y1-Y14 is the strain monitoring point, and each measuring point is equipped with bidirectional resistance strain gauges inside, outside and on the web side of the arch, which represent the radial and tangential stresses of the steel respectively (Figs. 4, 5).

3.1.1.5 Test Process

(1) Adjust the cylinder and the arch: install the hydraulic cylinder and the reaction sleeve plate, complete the hoisting of the loading beam, form the appropriate loading radius. Subsequently, the segmented arch is transported to the designated position by hanging according to the test requirements, and the arch frame is assembled (Figs. 6, 7).
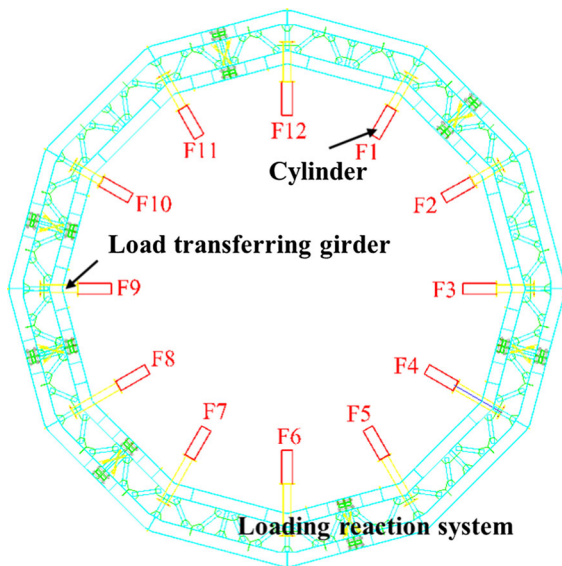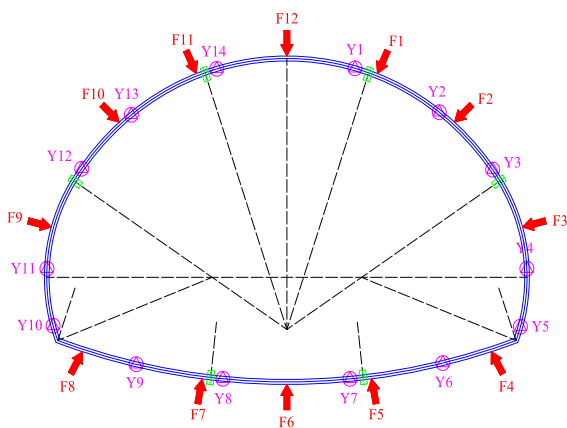
Fig. 4 Oil cylinder arrangement

Fig. 5 Monitoring point layout

(2) Installation of data monitoring and acquisition equipment: strain gauge is pasted on the measuring point of arch frame according to the test requirements and connected with the acquisition strain box through wire arrangement; displacement monitoring prism is fixed on the positioning plate through bolts or welding.

(3) Preloading: After the above-mentioned parts are installed, the load is slowly loaded through the hydraulic control system until the loaded beam is in close contact with the arch. At the same time, the pre-loading load should not exceed 5% of the theoretical failure load.

(4) Formal loading: According to the test scheme, the loading rate and holding time of the hydraulic cylinder are programmed to be controlled until the arch is destroyed and the experiment is completed (Fig. 8).

3.1.2 Numerical Test

Finite element analysis software ABAQUS is used to carry out numerical experiments. Figure 9 shows the effect of three-dimensional solid modeling and meshing. C3D8R entity unit modeling is adopted. The stress–strain relationship of reinforcing bar is based on a double-fold line model. The modulus of strengthening section is $0.01E_s$ and the elastic modulus of steel is E_s. $E_s = 1.97 \times 10^5$ MPa. According to the tensile test data, the yield strength of steel is 409 MPa. Specific numerical schemes refer to the related research (Wang et al. 2018; Li et al. 2018; Hongbin 2018).

In order to simulate the real laboratory test, the loading boundary conditions of the numerical test are consistent with the laboratory test. Twelve rigid loading beam models are set around the ring of the arch. Five loading beams at the bottom of the inverted arch are used as the fixed boundary conditions to support the arch, which is equivalent to the fixed foundation. The other seven loading beams are free boundary conditions. Displacement controlled loading is adopted.

3.2 Analysis of Test Results

3.2.1 Deformation and Failure Process and Shape of Arches in Laboratory Tests

At the initial stage of the loading process, no obvious deformation was observed. With the increase of radial force, the overall shape of the arch became flattened. Both sides of the upper and lower extrude inward, and the arch began to enter the working stage. At this moment, the arch components show no obvious local deformation.

Subsequently when the load is about to reach the ultimate value, the arch begins to deform rapidly, bending occurs at the bottom of the arch, curvature of the arch foot increases significantly. Since the torsional strength of I-shape arch is relatively low, local distortion occurs as the component reached the

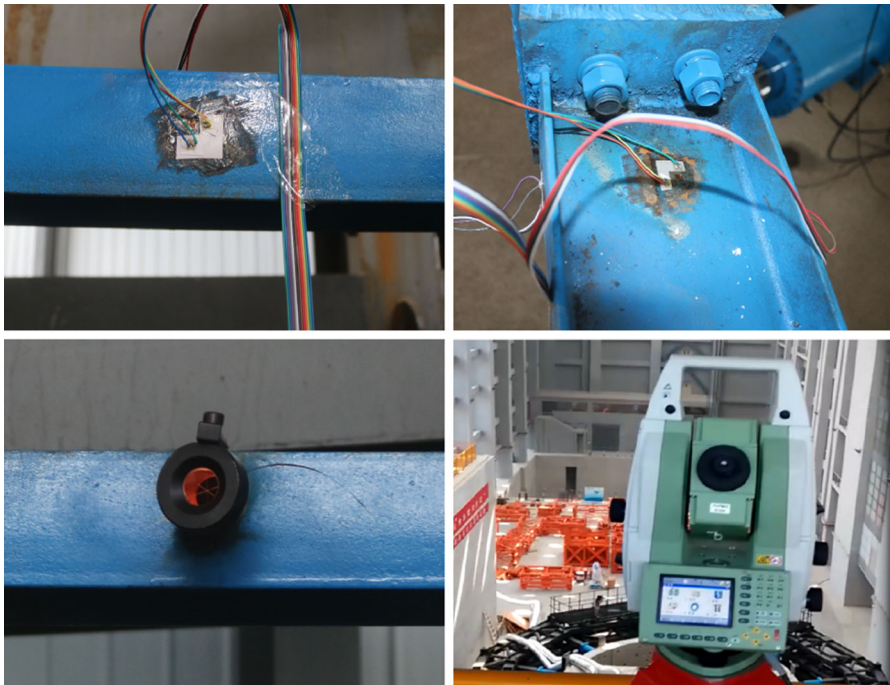**Fig. 6** Placement result of arch

Fig. 7 Monitoring arrangement of strain and displacement

ultimate strength at the arch foot. Then the deformation of the arch crown extruded inward as a whole, but the radian does not change significantly.

Up to the end of the test, the arch presents the instability deformation pattern of "crown sinking, arch waist convex, arch foot twisted" (Fig. 10).

3.2.2 Numerical Test of Deformation and Buckling of Arches

The deformation form of the arch frame obtained by ABAQUS numerical test is basically consistent with the laboratory test results. The crown of the arch frame is extruded inward as a whole, and the waist and foot of the arch are obviously convex. The test results show
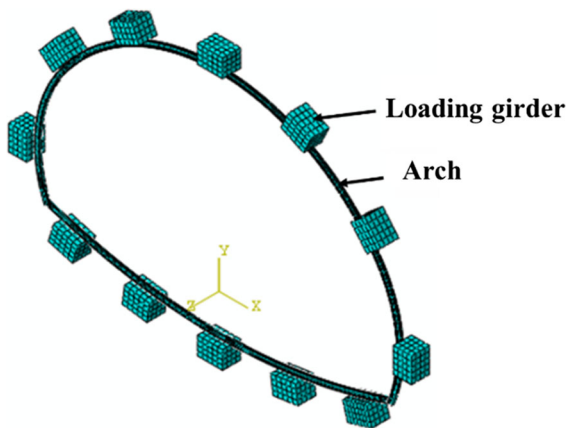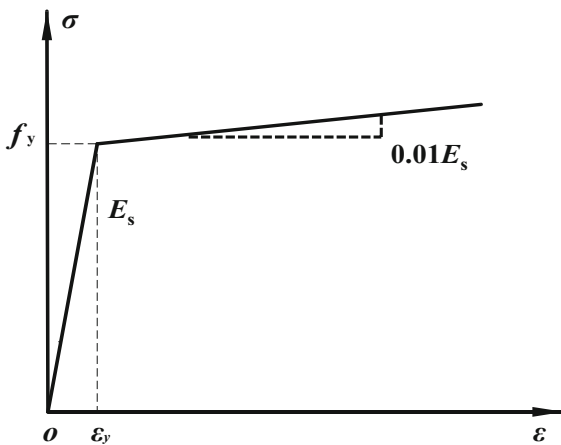
Fig. 8 Numerical test model

Fig. 9 Stress–strain relation curve

that the numerical test is in good agreement with the laboratory test (Fig. 11).

4 Stability Analysis of Arch Under Spatial Combination Condition

In order to further study the load-bearing mechanism and mechanical characteristics of arch under spatial combination state, based on the numerical test scheme mentioned above, three arch frames are combined by longitudinal connecting steel bars, and the numerical tests of arches under spatial combination state are carried out.

4.1 Test Situation

The constitutive relationship of longitudinal connection steel is listed in Sect. 3.1.2. The Analysis model of arch under spatial combination state is shown in Fig. 12. The arch and longitudinal connecting bar are bonded by tie contact, and the overlap length takes the section width of the arch (Figs. 13, 14).

The boundary conditions and loading modes of the model are consistent with that of the single arch numerical simulation test. The longitudinal displacements of the internal and external arches are constrained, and the spatial displacement of the middle arch is not constrained.

4.2 Analysis of Test Results

As the skeleton of initial support, the stability of arch and longitudinal connection determines the bearing capacity of initial support system. The numerical results show that the arch frame does not show obvious instability deformation under the constraint of longitudinal connection steel bar, and the stress distribution in the arch is obviously different from that of the single arch at the end of loading process. It can be seen that the bearing capacity of arch is fully exerted, and the displacement of arch crown is obviously reduced.

5 Research on Influence Mechanism of Spatial Layout Parameters of Arch Frame

In order to understand the influence of different combination spacing, different longitudinal connection spacing state on the bearing capacity of arch under combinational state, comparison scheme is set, and the specific factors are shown in Table 1. The design cost W of arch is defined as the total steel content (kg) of arch and longitudinal connection steel bar in every 10 m supporting section, and the design economic index β of arch frame is defined as the ratio of the bearing capacity F of combined arch to the design cost W of arch frame.

5.1 Influence of Arch Spacing on Its Bearing Capacity

The bearing capacity of combined arch has a linear relationship with the distance between the two

Fig. 10 Deformation of arch

(a) Before the test

(b) After the test

(c) Left arch leg deformed

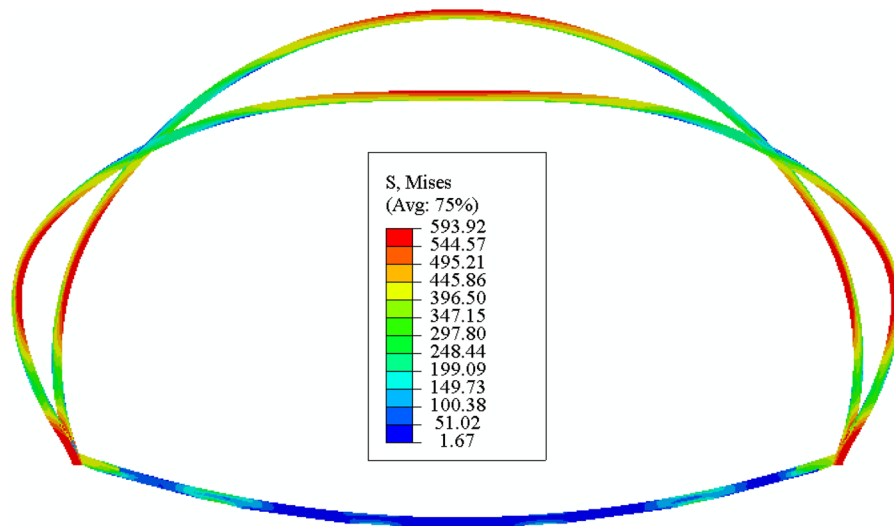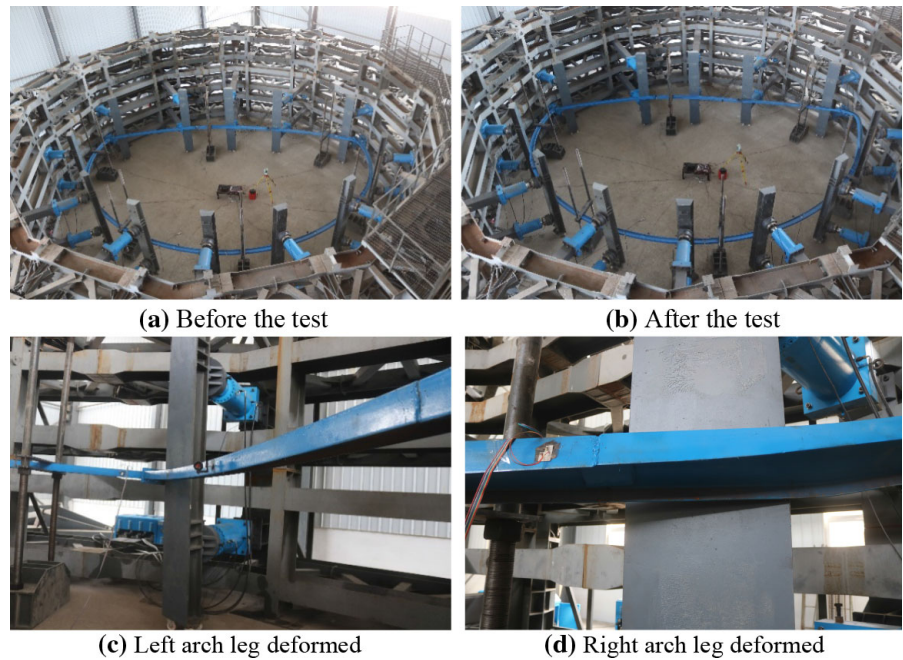**(d)** Right arch leg deformed

Fig. 11 Deformation of arch by numerical calculation

structures, and the effect of fitting degree $R^2 = 0.991$ is better. The bearing capacity of the combined arch decreases linearly with the increase of the distance between the two structures. When the combined spacing is 0.4, 0.6, 0.8, 1.0, 1.2 and 1.4 m, the bearing capacity is 3.92, 3.76, 3.59, 3.44, 3.28 and 3.14 times of single arch respectively, and the economic indexes is shown in Fig. 15.

It can be seen that the combined bearing effect of arches is obvious, and the spacing of arches can magnify the bearing capacity of the combined structure. It shows that the multi-arch has parallel effect, which leads to the increase of the strength and the bearing capacity of the combined structure (Figs. 16, 17).
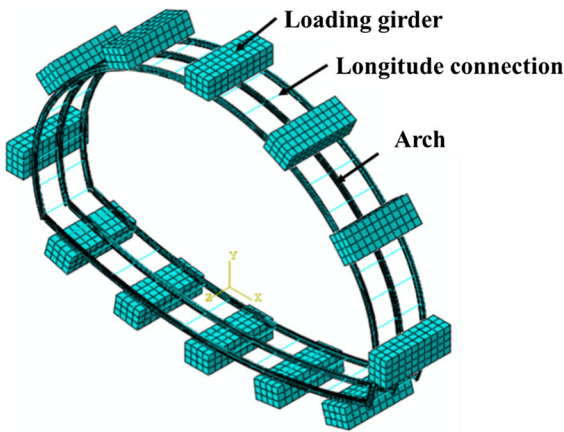
Fig. 12 Numerical test model of combined arch structure

5.2 Influence of Longitudinal Connection Spacing on Its Bearing Capacity

There is a logarithmic relationship between the bearing capacity of combined arch structure and the distribution spacing of longitudinal connection, and the effect of fitting degree $R^2 = 0.991$ is better. When the spacing is 0.5, 1.0, 1.5, 2.0 and 2.5 m, the bearing capacity is 3.63, 3.44, 3.32, 3.27 and 3.23 times of single arch respectively. The economic index is shown in Fig. 18.

When the spacing of distribution is less than 1.5 m, the bearing capacity of combined arch structure decreases obviously with the increase of the spacing

(a) Arch spacing 0.4m

(b) Arch spacing 0.6m

(c) Arch spacing 0.8m

(d) Arch spacing 1.0m

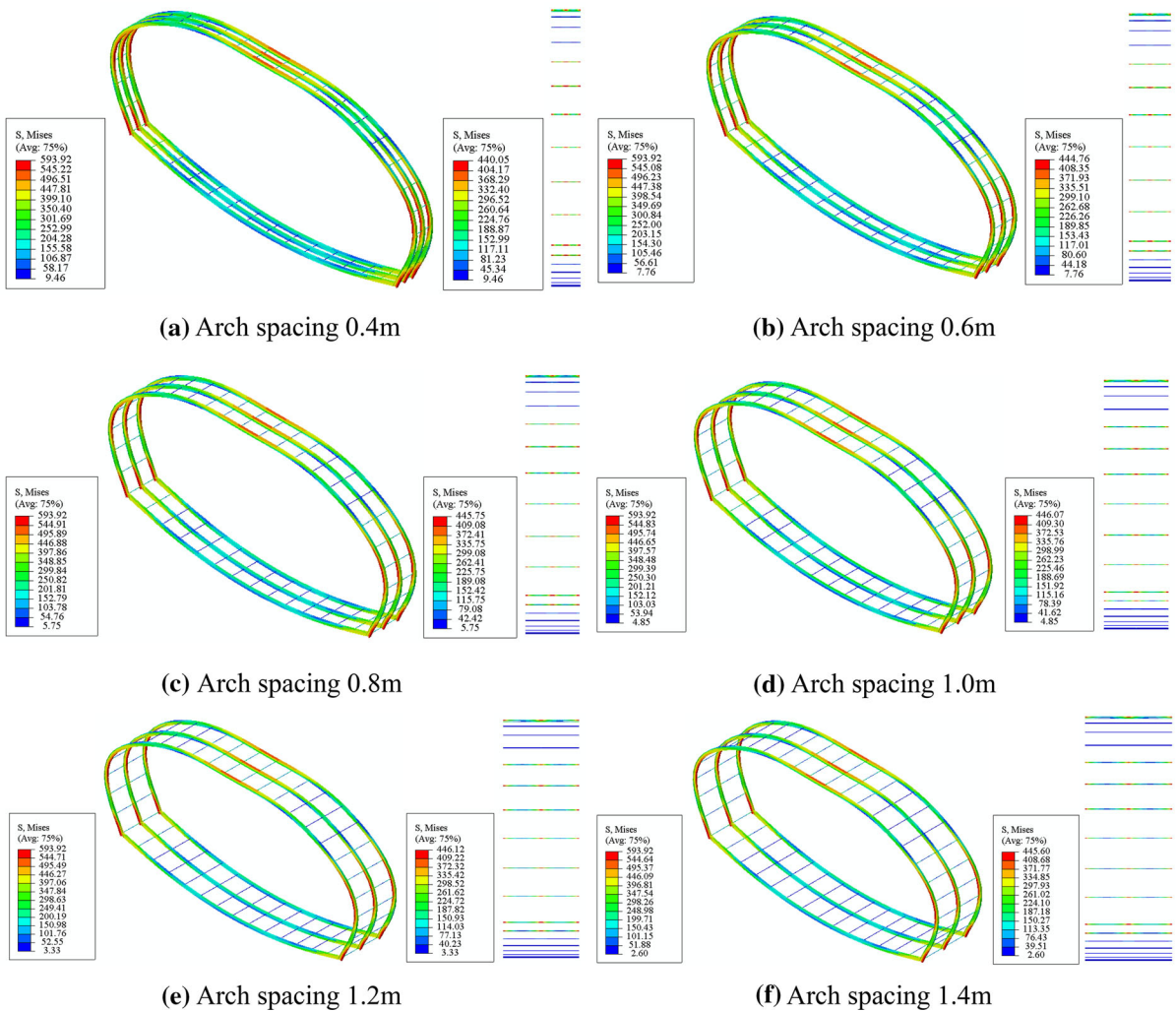**(e)** Arch spacing 1.2m

(f) Arch spacing 1.4m

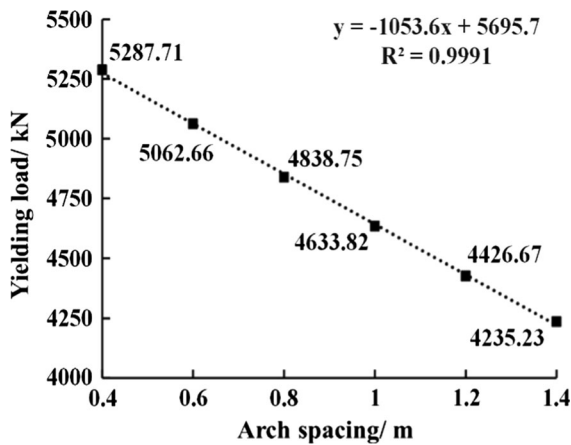Fig. 13 Arch stress nephogram of different arch spacing

Fig. 14 Influence curve of arch spacing on the bearing capacity of arch

Table 1 Factor levels of numerical tests

Number	Arch spacing (m)	Longitudinal connection spacing (m)
1	0.4	0.5
2	0.6	1.0
3	0.8	1.5
4	1.0	2.0
5	1.2	2.5
6	1.4	–
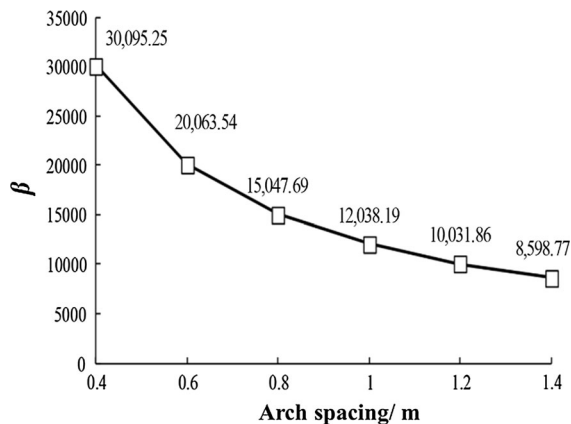
Fig. 15 Influence curve of arch spacing on the economic index

of longitudinal connection. When the spacing of distribution is more than 1.5 m, the decreasing trend of the bearing capacity of combined arch structure decreases gradually with the increase of the spacing of

longitudinal connection distribution. There is a certain scope of influence.

From the above analysis, it can be seen that the joint bearing effect between arches is obvious, and the longitudinal connection enlarges the bearing capacity of combined arch structure. It shows that the longitudinal connection can have a series effect on combined arch, resulting in the increase of the stiffness of combined structure and the enhancement of longitudinal stability. However, when the longitudinal connection spacing exceeds 1.5 m, the bearing capacity of the combined arch structure will be reduced (Fig. 19).

5.3 Coupling Action Rule Between Arch Joint Spacing and Longitudinal Connection Spacing

As can be seen from Fig. 19, the difference of arch bearing capacity under different longitudinal connection spacing becomes smaller and smaller with the increase of arch spacing, and the difference between the maximum and the minimum is 10 times. However, with the increase of longitudinal connection spacing, the difference of bearing capacity between different arch combinations under different working conditions has little change, only less than one time difference. It can be seen that the influence of arch combination spacing on the bearing capacity of combined arch is more obvious than that of longitudinal connection distribution spacing. But the longitudinal connection spacing is easier to control than that of arch spacing.

5.4 Design Advice

In the design process, the initial support system should not be overly reinforced, and it should be given full consideration on strength, economy and construction convenience as selecting arch spacing and longitudinal connection spacing.

Since the influence of arch spacing on the bearing capacity of combined arch is more obvious than that of longitudinal connection distribution spacing, while the longitudinal connection spacing is easier to control than that of arch spacing, designers should firstly select the spacing of arches according to the general situation of the engineering, and then the longitudinal connection spacing should be increased or reduced based on the calculation of support strength.

(a) Rebar spacing 0.5 m

(b) Rebar spacing 1.0 m

(c) Rebar spacing 1.5 m

(d) Rebar spacing 2.0 m
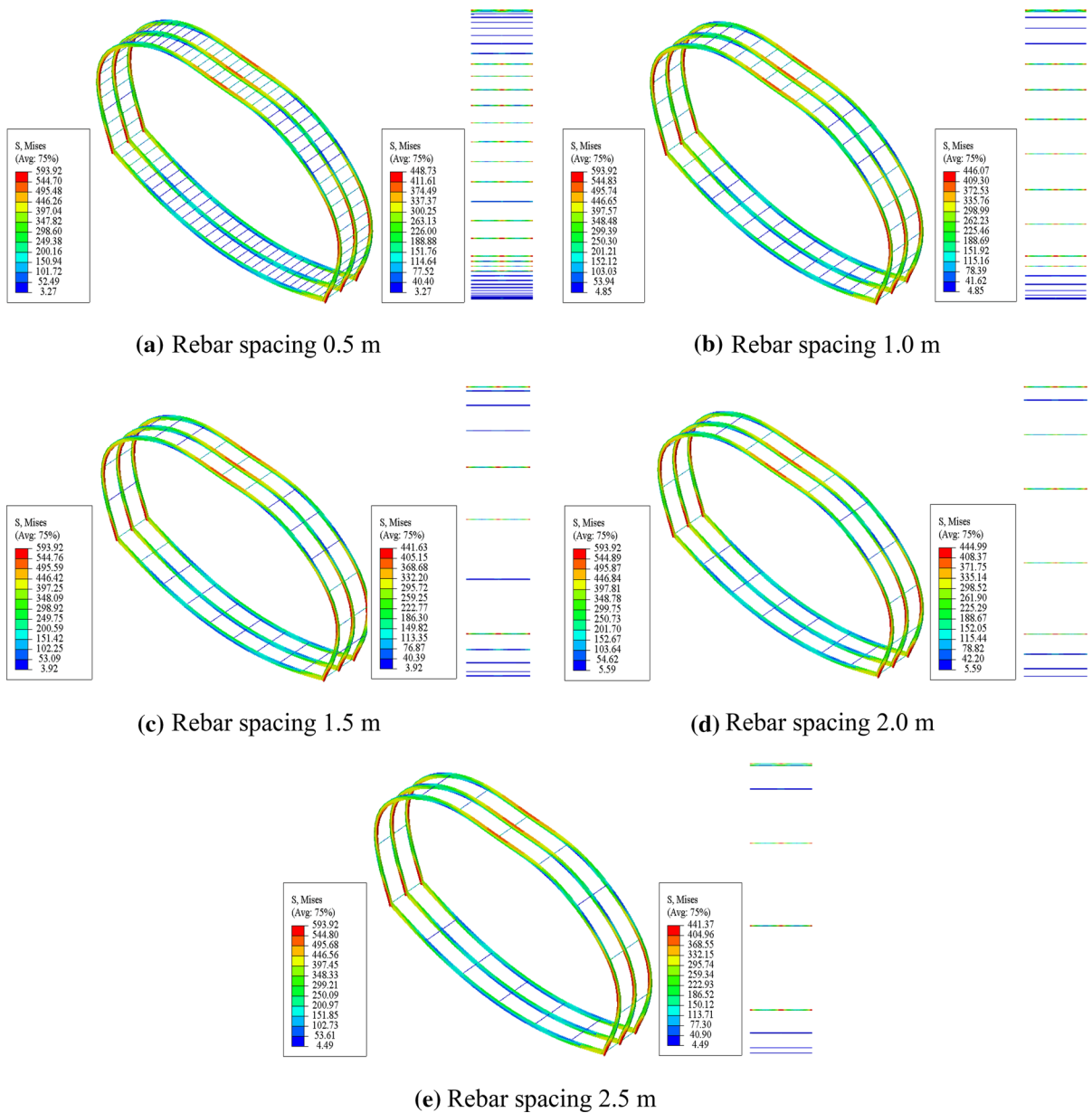
(e) Rebar spacing 2.5 m

Fig. 16 Arch stress nephogram with different longitudinal connection spacing

Reasonable design of spatial layout parameters of arch is the key to make full use of arch bearing capacity.

6 Conclusion

(1) The influence of arch spacing and longitudinal connection spacing on arch bearing capacity is remarkable. Parallel action exists between arch frames and series action between longitudinal connections, which results in the increase of longitudinal stiffness and strength of combined structures and enlarges the bearing capacity of single arch frame, which is 3.14–3.92 times of single arch frame.

(2) With the increase of the spacing of arch frame combination, the difference of bearing capacity between different longitudinal connection
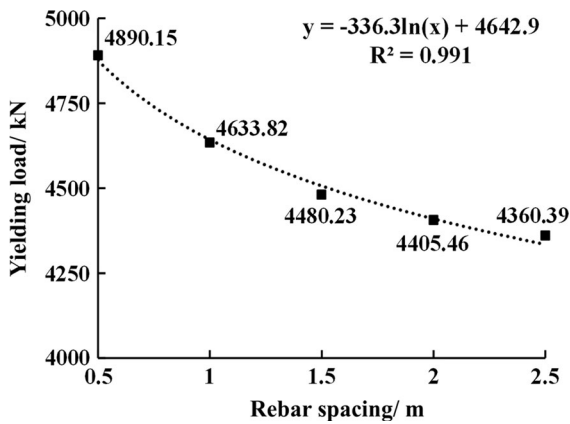
Fig. 17 Influence curve of longitudinal connection spacing on bearing capacity of arch
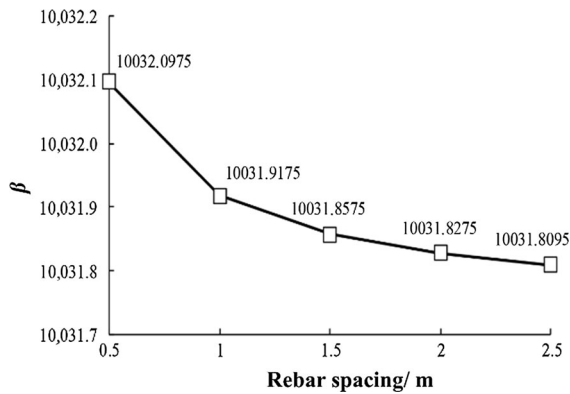

Fig. 18 Influence curve of longitudinal connection spacing on economic index
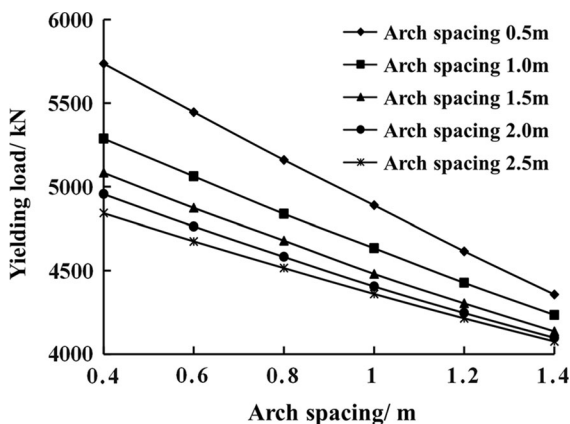

Fig. 19 Influence of coupling between arch spacing and longitudinal spacing on bearing capacity of combined structure

spacing becomes smaller and smaller, and the difference between the maximum and the minimum is 10 times. With the increase of longitudinal connection spacing, the difference of bearing capacity of different arch-frame combination spacing is not much different, less than one time. The influence of the spacing of arch frame combination on the bearing capacity of combined structure is more obvious than that of the spacing of longitudinal connection distribution. But the longitudinal connection spacing is easier to control than the arch spacing.

References

ANDERS (2005) A Laboratory testing of a new type of energy absorbing rock bolt. Tunn Undergr Space Technol 20(4):291–330

Dehua Z, Shihai L, Shoqiang R (2015) Research on selection of preliminary support for tunnel in high ground-stress soft-rock based on surrounding rock-support characteristic curve theory. China Civ Eng J 48(1):139–148

Gui-Jun W (2005) Mechanical state of jointed rock mass and support structure of large tunnel during construction process. Chin J Rock Mechan Eng 24(8):1328–1334

He M, Gong W, Wang J, Qi P, Tao Z, Shuai D, Peng Y (2014) Development of a novel energy-absorbing bolt with extraordinarily large elongation and constant resistance. Int J Rock Mech Min Sci 67:29–42

Høiena AH, Nilsen B, Olsson R (2019) Main aspects of deformation and rock support in Norwegian road tunnels. Tunn Undergr Space Technol 86:262–278

Hongbin C (2018) Research on bearing mechanism of arch primary support for super large section tunnel [Dissertation]. Shandong University, Jinan

Kang YS, Liu QS, Gong GQ, Wang HC (2014) Application of a combined support system to the weak floor reinforcement in deep underground coal mine. Int J Rock Mech Min Sci 71:143–150

Kezhong WANG, Yaoru LIU, Yupei WANG, Feng LIN, Changyang YU (2014) Study of deformation characteristics of compound support steel arch and surrounding rock stability in diversion tunnel. Chin J Rock Mech Eng 33(2):217–224

Kun JIANG, Cai-chu XIA, Yue-wei BIAN (2012) Optimal analysis of construction schemes of small space tunnel with Bidirectional Eight Traffic Lanes in Jointed Rock Mass. Rock Soil Mech 2012(03):841–847

Li SC, Lu W, Wang Q, Sun HB, Jiang B, Qin Q (2018) Study on failure mechanism and mechanical properties of casing joints of square steel confined concrete arch. 92:539–552

Li-chao HE, Meng-shu WANG, Yu-jie LI (2013) Supporting technology for shallow large-span neighborhood loess tunnel. Rock Soil Mech 34(S2):306–310

Liping LI, Shucai LI, Yong ZHAO et al (2012) Spatial deformation mechanism and load release evolution law of surrounding rock during construction of super-large section tunnel with soft broken surrounding rock masses. Chin J Rock Mechan Eng 10:2109–2118

Qing-biao WANG, Jin-quan JIANG, Lin-hai LU et al (2013) Simulation study on the influence of different excavation methods on the close overlap tunnel. Chin J Rock Mechan Eng 2013(10):2079–2087

Ranjbarnia M, Rahimpour N, Oreste P (2018) A simple analytical approach to simulate the arch umbrella supporting system in deep tunnels based on convergence confinement method. Tunn Undergr Space Technol 82:39–49

Sharifzadeh M, Kolivand F, Ghorbani M, Yasrobi S (2013) Design of sequential excavation method for large span urban tunnels in soft ground-Niayesh tunnel. Tunn Undergr Space Technol 35:178–188

Tiezhu Z (2015) Analysis of mechanical response of four-lane small clear spacing highway tunnel with super-large cross-section. China Civ Eng J S1:302–305

Wang Q, Jiang B, Li SC, Wang DC, Wang FQ, Li WT, Ren YX, Guo NB, Shao X (2016) Experimental studies on the mechanical properties and deformation & failure mechanism of U-type confined concrete arch centering. Tunn Undergr Space Technol 51:20–29

Wang Q, Pan R, Jiang B, Li SC, He MC, Sun HB, Wang L, Qin Q, Yu HC, Luan YC (2017) Study on failure mechanism of roadway with soft rock in deep coal mine and confined concrete support system. Eng Fail Anal 81:155–177

Wang Q, Jiang B, Pan R, Li S, He M, Sun H, Qin Q, Yu H, Luan Y (2018) Failure mechanism of surrounding rock with high stress and confined concrete support system. Int J Rock Mech Min Sci 102:89–100

Zheng-bin XI, Cang JIAO, Lian-shan WANG et al (2006) Analysis of characteristic of soft surrounding rock deformation for super large section tunnel excavation. ConstrTechnol S1:50–51